Conducting Copolymers of Pyridine with Thiophene, *N*-Methylpyrrole, and Selenophene

Ieuan H. Jenkins,† Ulrike Salzner, and Peter G. Pickup*

Department of Chemistry, Memorial University of Newfoundland, St. John's, Newfoundland, A1B 3X7, Canada

Received March 26, 1996. Revised Manuscript Received July 24, 1996⊗

A series of three-ring heteroaromatic compounds consisting of a pyridine central ring and thiophene, selenophene, or *N*-methylpyrrole outer rings, and their polymers have been investigated. Differences in redox potentials and electronic absorbance spectra of the three-ring monomers have been interpreted with the aid of HOMO and LUMO energies from ab initio calculations. Both p- and n-doping of the polymers were investigated electrochemically in acetonitrile. In all cases, the p-doped states were not stable, and measured conductivities were well below intrinsic values. In most cases, the n-doped states were more stable, but conductivities were very low.

Introduction

The synthesis and investigation of π-conjugated copolymers with structures **A** and **B** has attracted considerable interest in recent years.[1] The wide range of

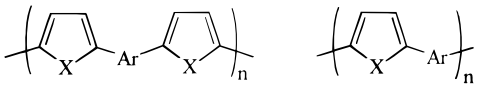

A **B**

aromatic building blocks that can be used offer considerable opportunities for development of novel conductive materials. In addition, the well-defined monomer sequences in these structures are attractive for fundamental studies aimed at understanding the electronic structures of conducting polymers. Type **A** polymers are normally obtained by electrochemical or chemical oxidation of the corresponding three monomer unit compound with linkages occurring predominantly through the 2,5-positions. Thiophene has generally been used as the electrochemically polymerizable end group, although pyrrole can also be used.[2] The central units employed include phenylene,[3−5] naphthalene,[6] pyridine,[3] thiazole,[7] pyrrole,[8,9] furan,[10] and benzo[*c*]thiophene.[11,12] Type **B** polymers, on the other hand, are usually obtained by a chemical coupling route, although poly(thienylpyrrole) has been obtained by electrochemical synthesis.[13] Examples of the pairings seen in type **B** polymers are, thiophene−phenylene,[14−17] selenophene−phenylene,[15] thiophene−pyridine,[15,18,19] and thiophene−pyrrole.[14,17]

Our interest in this area lies with the incorporation of donor nitrogen atoms into the π-conjugated backbone of the polymer. These nitrogen atoms can act as binding sites for transition-metal ions and facilitate electronic coupling between the metal ion and the π system of the polymers. Novel electronic, optical, and electrochemical properties are expected to arise from such interactions.[20−22]

Previously we reported the incorporation of 4,4′-dimethyl-2,2′-bithiazole moieties into a copolymer with thiophene.[23] Here we report results on a series of type **A** polymers, based on structures **1**−**4**, containing pyridine as the central unit. There have been several

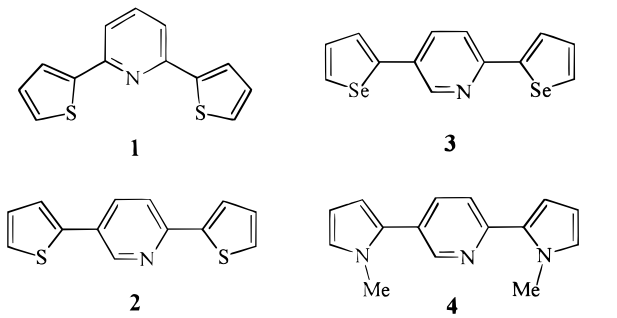

1 **3**

2 **4**

† Present Address: BAS Technicol, Adcroft Street, Higher Hillgate, Stockport, Cheshire, SK1 3HZ, UK.

* To whom correspondence should be addressed.

⊗ Abstract published in *Advance ACS Abstracts,* September 1, 1996.

(1) Krivoshei, I. V.; Skorobogatov, V. M. *Polyacetylene and Polyarylenes. Synthesis and Conductive Properties*; Gordon and Breach: Philadelphia, 1991; Polymer Monographs, Vol. 10.

(2) Reynolds, J. R.; Katritzky, A. R.; Soloducho, J.; Belyakov, S.; Sotzing, G. A.; Pyo, M. *Macromolecules* **1994**, *27*, 7225−7227.

(3) Tanaka, S.; Sato, M.-A.; Kaeriyama, K. *J. Macromol. Sci.-Chem.* **1987**, *A24*, 749−761.

(4) Pelter, A.; Maud, J. M.; Jenkins, I. H.; Sadeka, C.; Coles, G. *Tetrahedron Lett.* **1989**, *30*, 3461.

(5) Ruiz, J. P.; Dharia, J. R.; Reynolds, J. R.; Buckley, L. J. *Macromolecules* **1992**, *25*, 849−860.

(6) Tanaka, S.; Kaeriyama, K. *Polym. Commun.* **1990**, *31*, 172−175.

(7) Tanaka, S.; Kaeriyama, K. *Makromol. Chem., Rapid Commun.* **1988**, *9*, 743−748.

(8) McLeod, G. G.; Mahboubian-Jones, M. G. B.; Pethrick, R. A.; Watson, S. D.; Truong, N.; Galin, J. C.; Francois, J. *Polymer* **1986**, *27*, 455−458.

(9) Ferraris, J. P.; Andrus, R. G.; Hrncir, D. C. *J. Chem. Soc., Chem. Commun.* **1989**, 1318−1320.

(10) Ferraris, J. P.; Hanlon, T. P. *Polymer* **1989**, *30*, 1319−1327.

(11) Lorcy, D.; Cava, M. P. *Adv. Mater.* **1992**, *4*, 562−564.

(12) Musmanni, S.; Ferraris, J. P. *J. Chem. Soc., Chem. Commun.* **1993**, 172−174.

(13) Naitoh, S.; Sanui, K.; Ogata, N. *J. Chem. Soc., Chem. Commun.* **1986**, 1348−1350.

(14) Bracke, W. *J. Polym. Sci., Part A: Polym. Chem.* **1972**, *10*, 975−981.

(15) Montheard, J. P.; Pascal, T.; Seytre, G.; Steffan-Boiteaux, G.; Douillard, A. *Synth. Met.* **1984**, *9*, 389−396.

(16) Pelter, A.; Rowlands, M.; Jenkins, I. H. *Tetrahedron Lett.* **1987**, *28*, 5213.

(17) Pouwer, K. L.; Vries, T. R.; Havinga, E. E.; Meijer, E. W.; Wynberg, H. *J. Chem. Soc., Chem. Commun.* **1988**, 1432−1433.

(18) Yamamoto, T.; Shimura, M.; Osakada, K.; Kubota, K. *Chem. Lett.* **1992**, 1003−1004.

(19) Maruyama, T.; Kubota, K.; Yamamoto, T. *Chem. Lett.* **1992**, 1827−1830.

S0897-4756(96)00207-4 CCC: $12.00

reports on the electropolymerization of 2,6-bis(2-thienyl)pyridine (2,6-th_2py, **1**)[3,7,24] and 2,5-bis(2-thienyl)-pyridine (2,5-th_2py, **2**),[3,7] and poly(2,6-th_2py) has been investigated as a substrate for metal ion coordination.[24] As far as we know, 2,5-bis(2-selenienyl)pyridine (2,5-sel_2py, **3**), and 2,5-bis(1-methyl-2-pyrrolyl)]pyridine (2,5-mp_2py, **4**) have not previously been reported. We report here a comprehensive experimental and theoretical comparison of these four materials and their polymers. Their reductive electrochemistry and n-doping of the polymers is reported for the first time. The n-doping (reduction) of π-conjugated polymers has been attracting increasing attention recently, because of envisaged applications in microelectronics and supercapacitors.[25−27] Pyridine-containing polymers have been of particular interest as n-doped organic semiconductors.[27−29]

Experimental Section

Syntheses. The syntheses of **1** and **2** have been previously reported.[3,24,30] In our laboratory they were made both by the Negishi[24,31] type cross-coupling of 2-thienylzinc chloride and the Suzuki[32] style cross-coupling of 2-thienylboronic acid with the corresponding pyridine dibromide. Only the latter route, which has not previously been reported for these compounds, will be described. An analogous procedure worked well for **3** but was unsuccessful for **4**. The latter compound was therefore prepared using 1-methyl-2-pyrrolylzinc chloride.

Reagents and Instruments. 1-Methylpyrrole, tetrakis-(triphenylphosphine)palladium(0), 2,6-bromopyridine, 2,5-dibromopyridine, 2-thienyllithium, and selenophene were all obtained from Aldrich and used without further purification. Zinc chloride (Anachemia) was dried at 120 °C under vacuum for at least 4 h prior to use. THF (Anachemia) was dried by refluxing over calcium hydride (Fisher) prior to use. DME (Aldrich, 99%) and chloroform were used without further purification.

Melting points were obtained using a Fisher-John's hot-stage apparatus and are uncorrected. ^{1}H NMR spectra were all recorded at 300 MHz using TMS as a standard.

2,6-Bis(2-thienyl)pyridine (1). A mixture of 2-thienylboronic acid[33] (4.9 g, 38 mmol), 2,6-dibromopyridine (3.0 g, 13 mmol), $Pd(PPh_3)_4$ (0.5 g, 0.43 mmol), sodium hydrogen carbonate (3.2 g, 38 mmol), THF (120 mL), and water (20 mL) was refluxed under nitrogen for 24 h. The product was extracted into ether which was then dried with magnesium sulfate and removed under reduced pressure. Purification on a silica column with 1:1 hexane/chloroform gave 2.5 g of product (82% yield). The melting point (78−79 °C) and ^{1}H NMR spectrum agreed with literature values.[3,24]

2,5-Bis(2-thienyl)pyridine (2). The procedure was the same as described above for **1**, except that (a) 8:1 1,2-dimethoxyethane (DME)/water was used as the solvent, (b) 100 mL of 5 M HCl was added to the reaction mixture before extraction with ether, (c) the ether extract was washed with saturated $NaHCO_3$(aq) and then water, and (d) 4:1 hexane/chloroform was used as the eluent for chromatography. The melting point (146−147 °C) and ^{1}H NMR spectrum agreed with literature values.[3] The yield was 61%

2,5-bis(2-selenienyl)pyridine (**3**). A mixture of 2-selenopheneboronic acid[34] (1.0 g, 5.7 mmol), 2,5-dibromopyridine (0.70 g, 2.9 mmol), $Pd(PPh_3)_4$ (0.10 g, 0.08 mmol), sodium hydrogen carbonate (0.50 g, 5.7 mmol), DME (30 mL) and water (5 mL) was refluxed under nitrogen for 24 h. The reaction mixture was then added to water (50 mL) and extracted with ether. After drying with magnesium sulfate and removal of the ether under reduced pressure, the crude product was purified on a silica/hexane column. Melting point = 150 °C.

^{1}H NMR (300 MHz, $CDCl_3$, σ (ppm)) 8.74 (1H, dd, $J(3-6)$ = 0.6 Hz, $J(4,6)$ = 2.3 Hz, H-6), 8.17 (1H, dd, $J(3'-5')$ = 1.0 Hz, $J(3'-4')$ = 5.6 Hz, H-3′), 8.02 (1H, dd, $J(3''-5'')$ = 1.0 Hz, $J(3''-5'')$ = 5.6 Hz, H-3″), 7.81 (1H, dd, $J(4-3)$ = 8.3 Hz, H-4), 7.75 (1H, dd, $J(4'-5')$ = 3.9 Hz, H-5′), 7.65 (1H, dd, H-3), 7.53 (1H, dd, $J(4''-5'')$ = 3.8 Hz, H-5″), 7.36 (2H, m, H-4′ and H-4″); ms *m*/*z* 339 (M^+, 100%) 337 (97), 336 (43), 335 (65), 258 (14). Anal. Found: C, 46.44%; H, 2.79%; N 4.10%. Calculated for $C_{13}H_9NSe_2$: C, 46.31%; H, 2.69%; N, 4.15%.

2,5-Bis(1-methyl-2-pyrrolyl)pyridine (4). A pentane solution of *tert*-butyllithium (25 mmol) was added slowly to a stirred solution of 1-methylpyrrole (2.0 g, 25 mmol) in THF (20 mL) at −70 °C.[35] The mixture was allowed to warm and after 0.5 h at room temperature was added to a solution of zinc chloride (3.4 g, 25 mmol) in THF (25 mL). This mixture was stirred at room temperature for 1 h, and then the resulting 1-methyl-2-pyrrolylzinc chloride solution was added to a mixture of the catalyst, tetrakis(triphenylphosphine)palladium-(0) (0.35 g, 0.30 mmol), and 2,5-dibromopyridine (1.43 g, 6 mmol). After 24 h at room temperature, the reaction mixture was quenched with 1 M ammonium chloride (aq, 80 mL). The aqueous layer was extracted with ether, and the combined organic fractions were washed with water, dried with $MgSO_4$, and concentrated at reduced pressure. Purification on a silica column with 20% ethyl acetate in petroleum ether (40−60 °C) gave the desired product in 70% yield (melting point = 92−93 °C). ^{1}H NMR (300 MHz, $CDCl_3$, σ (ppm)) 8.59 (1H, dd, $J(3-6)$ = 0.7 Hz, $J(4-6)$ = 2.3 Hz, H-6), 7.71 (1H, dd, $J(3-4)$ = 8.4 Hz, H-4), 7.61 (1H, dd, H-3), 6.78 (2H, m, H-5′ and H-5″), 6.63 (1H, dd, $J(3'-5')$ = 1.8 Hz, $J(3'-4')$ = 3.9 Hz, H-3′), 6.26 (1H, dd, $J(3''-5'')$ = 1.8 Hz, $J(3''-4'')$ = 3.6 Hz, H-3″), 6.11 (2H, m, H-4′ and H-4″), 4.00 (3H, s, −Me′), 3.66 (3H, s, −Me″); ms *m*/*z* 237 (M^+, 100%) 236 (90), 220 (9), 157 (10), 118 (12). Anal. Found: C, 75.59; H, 6.37; N, 17.71; M^+ 237.1261. Calculated for $C_{15}H_{15}N_3$: C, 75.90; H, 6.37; N, 17.71; M^+ 237.12652.

Electrochemistry. Electrochemical experiments were performed in conventional three-compartment glass cells at room temperature. The working electrode was a 0.0052 cm^2 Pt disk sealed in glass and the reference electrode was a saturated sodium chloride calomel electrode (SSCE). Tetraethylammonium perchlorate (Fluka, >99%), tetrabutylammonium hexafluorophosphate (Fluka, 98%), chloroform (Caledon, spectroscopic grade), and acetonitrile (Fisher, HPLC grade) were used as received.

Impedance measurements were carried out with a Solartron frequency response analyzer (Model 1250) and a Solartron electrochemical interface (Model 1286). All data were collected and analyzed using an IBM compatible microcomputer and ZPLOT software (Scribner Associates Inc.).

Computational Methods. Geometries of monomers **1**−**4** and of the benzene analogues, 1,5-bis(2-thienyl)benzene (**1a**) and 1,4-bis(2-thienyl)benzene (**2a**), were fully optimized em-

(20) Wolf, M. O.; Wrighton, M. S. *Chem. Mater.* **1994**, *6*, 1526−1533.
(21) Nishihara, H.; Shimura, T.; Ohkubo, A.; Matsuda, N.; Aramaki, K. *Adv. Mater.* **1993**, *5*, 752−754.
(22) Yamamoto, T.; Yoneda, Y.; Maruyama, T. *J. Chem. Soc., Chem. Commun.* **1992**, 1652−1654.
(23) Jenkins, I. H.; Pickup, P. G. *Macromolecules* **1993**, *26*, 4450−4456.
(24) Higgins, S.; Crayston, J. A. *Synth. Met.* **1993**, *55*, 879−883.
(25) Guerrero, D. J.; Ren, X. M.; Ferraris, J. P. *Chem. Mater.* **1994**, *6*, 1437−1443.
(26) Shi, G. Q.; Yu, B.; Xue, G.; Shi, J. B.; Li, C. *J. Chem. Soc., Chem. Commun.* **1994**, 2549−2550.
(27) Onoda, M. *J. Appl. Phys.* **1995**, *78*, 1327−1333.
(28) Yamamoto, T.; Ito, T.; Sanechika, K. *Synth. Met.* **1988**, *25*, 103−107.
(29) Miyamae, T.; Yoshimura, D.; Ishii, H.; Ouchi, Y.; Saki, K.; Miyazaki, T.; Koike, T.; Yamamoto, T. *J. Chem. Phys.* **1995**, *103*, 2738−2744.
(30) Tamao, K.; Kodama, S.; Nakajima, I.; Kumada, M. *Tetrahedron* **1982**, *38*, 3347.
(31) Negishi, E.; King, A. O.; Okuda, N. *J. Org. Chem.* **1977**, *42*, 1821.
(32) Miyaura, N.; Yanagi, T.; Suzuki, A. *Synth. Commun.* **1981**, *11*, 513.
(33) Hornfeldt, A.-B.; Gronowitz, S. *Ark. Kemi* **1963**, *21*, 239.
(34) Shabana, R.; Galal, A.; Mark, H. B.; Zimmer, H.; Gronowitz, S.; Hornfeldt, A.-B. *Phosphorus, Sulfur, Silicon* **1990**, *48*, 239−244.
(35) Minato, A.; Tamao, K.; Hayashi, T.; Suzuki, K.; Kumada, M. *Tetrahedron Lett.* **1981**, *22*, 5319−5322.

Table 1. Formal Potentials ($E^{\circ\prime}$) or Peak Potentials (E_{pa}) from Cyclic Voltammetry of Compounds 1−4 in CH_3CN Containing 0.05 M Bu_4NPF_6

	potential (V vs SSCE)	
monomer	oxidation, E_{pa}	reduction, $E^{\circ\prime}$
2,6-bis(2-thienyl)pyridine	+1.46	−2.26
2,5-bis(2-thienyl)pyridine	+1.35	−2.08
2,5-bis(2-selenienyl)pyridine	+1.27	−1.95
2,5-bis(1-methyl-2-pyrrolyl)]pyridine	+0.83	

ploying the local spin density approximation and Hay/Wadt pseudopotentials in connection with split-valence basis sets (LSDA/LANL2DZ). Geometries of **1**−**4** were also determined with a gradient-corrected functional using the same basis set (Becke3LYP/LANL2DZ). All calculation were carried out with G92/DFT.[36] Electronic structures were analyzed with the NBO method[37] as implemented in G92/DFT.

LSDA is known to underestimate HOMO−LUMO gaps.[38] The correlation corrected Becke3LYP functional leads to increases of the HOMO−LUMO gaps in our calculations of about 33%. This indicates that inclusion of correlation corrects the shortcomings of the LSDA method for the most part. Since the LANL2DZ basis set does not include polarization functions, we carried out further tests on **2** with all-electron calculations and the 6-31G* basis set. With both LSDA and Becke3LYP the C−S bond distances decreased by about 0.07 Å. The HOMO−LUMO gaps, however, which are our major concern here differed by no more than 0.1 eV, justified the use of the unpolarized basis sets for this purpose.

Results and Discussion

Properties of the Three-Ring Monomers. Cyclic voltammograms for compounds **1**−**4** in CH_3CN containing 0.05 M Bu_4NPF_6 all showed irreversible oxidation waves. Compounds **1**−**3** also showed reduction waves with corresponding reoxidation waves (almost reversible), while **4** could not be reduced in the accessible potential range (to −2.5 V). Formal or peak potentials from the voltammograms are listed in Table 1.

The experimental peak potentials for oxidation ($E_{pa,ox}$) correlate well with HOMO energies from Becke3LYP/LANL2DZ calculations (Figure 1A). Linear regression provides the relationship, $E_{pa,ox} = -0.70E_{HOMO} - 2.71$. The slope is presumably less than unity because of enhanced solvation and ion pairing of the higher energy cation radicals. There is also a correlation between the calculated LUMO energies and the experimental formal potentials for reduction (Figure 1B), although it is not so strong. A good correlation is not to be expected in this case because LUMO energies do not provide very good estimates for electron affinities. The approximate relationship from a linear regression analysis is $E_{red}^{\circ\prime} = -0.82E_{LUMO} - 3.75$.

Figure 2 shows electronic spectra of compounds **1**−**4** in $CHCl_3$. HOMO−LUMO energy gaps estimated from the wavelengths of absorption onset are listed in Table 2, together with values from cyclic voltammetry ($E_{pa,ox} - E_{red}^{\circ\prime}$) and from Becke3LYP/LANL2DZ calculations.

The selenophene compound exhibits the lowest HOMO−LUMO gap. The gap for the *N*-methylpyrrole

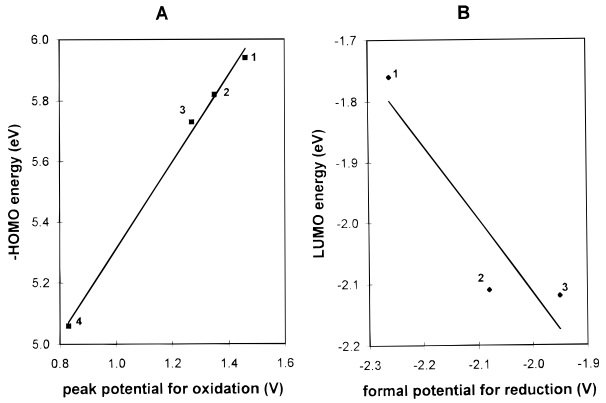

Figure 1. Plots of redox potentials vs calculated HOMO and LUMO energies for compounds **1**−**4**.

compound is slightly higher than for the 2,5-thiophene compound but lower than for the 2,6-thiophene compound. The theoretical HOMO−LUMO gaps are 0.3−0.7 eV higher than the optical and electrochemical gaps, while the electrochemical gaps are 0.02−0.2 eV higher than the optical gaps. The theoretical HOMO−LUMO energies reflect the trend in experimental gaps reasonably well, and so use of the results of Becke3LYP/LANL2DZ calculations to rationalize the experimental results appears to be justified.

The larger bandgap of **1** compared to **2** is mainly due to the higher lying LUMO of **1**. NBO analysis indicates that **1** has a larger total π-delocalization, but **2** exhibits stronger π-delocalization between the individual rings. The smaller HOMO−LUMO gap of **2** can therefore be attributed to a stronger coupling between the π-systems of the thiophene and pyridine rings, which increases conjugation along the chain.

Comparison of **1** and **2** with the parent benzene analogues, **1a** and **2a**, shows interesting similarities and differences. The calculated (LSDA/LANL2DZ) band-

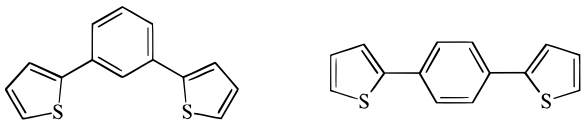

1a **2a**

gaps of **1** and **1a** and those of **2** and **2a** are virtually identical. The differences between the HOMO−LUMO gaps of **1** and **2** and of **1a** and **2a** are therefore identical (0.44 eV). The presence of a nitrogen atom leads to a decrease of the HOMO and of the LUMO of about 0.1 eV in **1** and of about 0.2 eV in **2**. The pyridine systems are therefore predicted to be more difficult to oxidize but easier to reduce than the benzene systems. For the benzene system the para isomer (**2a**), which has the lower bandgap, is 0.87 kcal/mol more stable than the meta isomer (**1a**). In contrast, for the pyridine system the meta isomer (**1**), which has the higher bandgap, is 2.09 kcal/mol more stable than the para isomer (**2**).

The sulfur and selenium systems, **2** and **3**, have similar bandgaps as well as similar HOMO and LUMO energies. Such similarities are found in general for sulfur and selenium compounds.

Although **2** and **4** have very similar bandgaps, **4** could not be reduced within the available potential range (>−

(36) Frisch, M. J.; Trucks, G. W.; Schlegel, H. B.; Gill, P. M. W.; Johnson, B. G.; Wong, M. W.; Foresman, J. B.; Robb, M. A.; Head-Gordon, M.; Replogle, E. S.; Gomperts, R.; Andres, J. L.; Raghavachari, K.; Blinkley, J. S.; Gonzales, C.; Martin, R. L.; Fox, D. L.; Defrees, D. J.; Baker, J.; Stewart, J. J. P.; Pople, J. A. *GAUSSIAN 92/DFT, Revision F.4*; Gaussian Inc.: Pittsburgh, 1992.

(37) Reed, A. E.; Curtiss, L. A.; Weinhold, F. *Chem. Rev.* **1988**, *88*, 899.

(38) Vogl, P.; Campbell, D. K. *Phys. Rev. B* **1990**, *41*, 12797−12816.

Table 2. HOMO−LUMO Energy Gaps for Compounds 1−4

monomer	optical gap (eV)	electrochemical gap (eV)	theoretical gap (eV) (Becke3LYP/LANL2DZ)
2,6-bis(2-thienyl)pyridine	3.43	3.72	4.18
2,5-bis(2-thienyl)pyridine	3.32	3.43	3.70
2,5-bis(2-selenienyl) pyridine	3.20	3.22	3.61
2,5-bis(1-methyl-2-pyrrolyl)pyridine	3.36		3.80

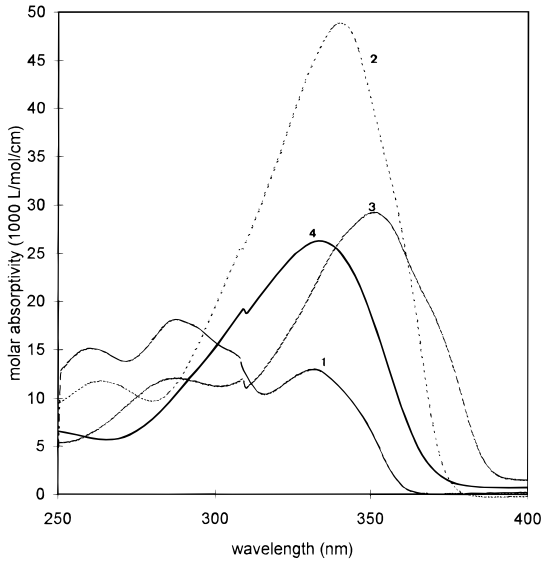

Figure 2. Electronic absorption spectra of compounds **1**−**4** in $CHCl_3$.

2.5 V). The calculated HOMO/LUMO energies show that the similar bandgaps of **2** and **4** are due to the fact that the HOMO and LUMO of **4** are both shifted to higher energies compared to those of **2** by ca. 0.8 eV. Since reduction of **2** requires a potential of −2.08 V (Table 1), a 0.8 V lower value for **4** would be outside the accessible potential range. Thus the high-lying LUMO of **4** accounts for the observation that **4** can not be reduced.

Polymerization of the Three-Ring Monomers. All four compounds polymerize in CH_3CN when the potential is cycled through the irreversible oxidation wave. Polymerization to give an electroactive polymer is indicated by the development of a reversible redox wave at lower potential than the initial oxidation wave. Polymer films for further study were most conveniently prepared at constant current. At 0.8 mA cm^{-2}, the potential rose quickly to a maximum, decayed slowly to a minimum (at E_{min} and t_{min}), and then began to rise continuously. Potentials and times for the minima are given in Table 3. The increase in potential after t_{min} is due to irreversible overoxidation of the polymer, which increases its resistance and redox potential.[39] Eventually the potential rises so high that the polymer film becomes totally deactivated. The thickness of high quality film that can be produced is therefore limited by t_{min}. Results from films prepared for times longer than t_{min} should be treated with caution because such films will have been overoxidized to some extent. t_{min} can be increased by increasing the monomer concentration or by decreasing the current density.

Electrochemistry of Polymers. All four polymers exhibit both p-doping (oxidative) and n-doping (reductive) electrochemistry. In general, the p-doped forms are less stable in CH_3CN than the n-doped forms, although the reverse is true for the pyrrole based polymer (poly-mp_2py). Approximate formal potentials from cyclic voltammetry are given in Table 4. Accurate values were difficult to obtain because of changes during cycling due to instability of the oxidized forms, and break-in phenomena for the reduced forms (see below). The reversible doping charges observed in cyclic voltammetry (Q_{cv}) were approximately 5% of the charge used for the polymerization (Q_{pol}) in most cases (Table 5). Due to instability of the highly doped polymers, the undoping charge observed in cyclic voltammetry goes through a maximum as the potential limit is increased (more negative for n-doping). The data given in Table 5 are estimates of this maximum undoping charge.

Polymerization of the three-ring monomers used here should involve approximately three electrons per molecule—two for the polymerization and one to dope the resulting polymer to the 30% level typical for polyheterocycles.[40] Doping/undoping by cyclic voltammetry should involve ca. one electron per three-ring unit in the polymer. The voltammetric charge (Q_{cv}) should therefore be ca. 30% of the polymerization charge (Q_{pol}) if the Coulombic efficiency of the polymerization is high. The much lower values reported in Table 5 can be attributed to a number of causes. Firstly, the polymerization efficiencies may be significantly lower than 100%. Although electrochemical polymerization of terthiophene occurs with high efficiency,[41] we have observed low efficiencies (ca. 40%) for four ring bis(thienyl)bithiazole compounds.[23] Current efficiencies of 56% and 73% have been reported for **1** and **2**, respectively.[3] Instability of the highly doped forms of all polymers is an important contributing factor to the low voltammetric charges in Table 5, particularly for p-doping. The very low Q_{cv} for p-doping of poly(2,5-Se_2py) is clearly due to the low stability of the p-doped form (see below). For n-doping, break-in (see below) may not have been complete and/or degradation will have occurred during break-in. Incomplete break-in was certainly a significant factor in the low Q_{cv} observed for n-doping of the poly(2,6-th_2py) sample, which exhibited a very slow break-in.

Pertinent details of the electrochemistries of each polymer are given in the following sections.

Poly[2,6-bis(2-thienyl)pyridine] (poly-1). Cyclic voltammograms for two films of poly(2,6-th_2py) are shown in Figure 3. Data for different films are used here to illustrate the p-doping and n- doping electrochemistries because the first film did not exhibit reversible n-doping after being p-doped. This type of "memory effect" was observed in several other instances, including cases where p-doping became irreversible following

(39) Gratzl, M.; Hsu, D.-F.; Riley, A. M.; Janata, J. *J. Phys. Chem.* **1990**, *94*, 5973−5981.

(40) Heinze, J. *Synth. Met.* **1991**, *41*−*43*, 2805−2823.

(41) Eales, R. M.; Hillman, A. R. *J. Electroanal. Chem.* **1988**, *250*, 219−223.

Table 3. Times (t_{min}) and Potentials (E_{min}) of Potential Minima during Electrochemical Polymerization at 0.8 mA cm^{-2}

monomer	concentration (mM)	t_{min} (s)	E_{min} (V vs SSCE)
2,6-bis(2-thienyl)pyridine	6.9	$100 < t_{min} < 180$	1.41
2,5-bis(2-thienyl)pyridine	6.2	>200	<1.27
2,5-bis(2-selenienyl) pyridine	5.8	no minimum	1.30 at 30 s
2,5-bis(1-methyl-2-pyrrolyl)pyridine	7.0	$50 < t_{min} < 100$	0.81

Table 4. Approximate Formal Potentials for the Polymers of Compounds 1−4 from Cyclic Voltammetry in CH_3CN Containing 0.05 M Bu_4NPF_6

	formal potential (V vs SSCE)	
monomer	oxidation	reduction
2,6-bis(2-thienyl)pyridine	+1.4	−1.75
2,5-bis(2-thienyl)pyridine	+1.1	−1.75
2,5-bis(2-selenienyl)pyridine	+1.1	−1.65
2,5-bis(1-methyl-2-pyrrolyl)pyridine	+0.9	−0.8

n-doping. It results, at least in part, from instability of the doped states.

The p-doping electrochemistry observed in Figure 3 (at potentials greater than +0.8 V) is similar to that previously reported for this polymer,[7,24] although in our experiments no clearly defined anodic peak could be observed without overoxidizing and deactivating the film. Scanning repeatedly into the p-doping wave caused it to gradually decrease and shift to higher potentials. This degradation in the electrochemical response became more rapid as the upper potential limit was increased. Clearly, p-doped poly(2,6-th$_2$py) has limited stability in CH_3CN. This can be attributed to a high reactivity of its cation radical or dication charge carriers with trace water in the electrolyte solution.[42] This high reactivity is presumably due to their restricted delocalization, which is also reflected in the high formal potential.

N-doping of poly(2,6-th$_2$py) requires a break-in period. For the film used in Figure 3, the current was negligible (<0.05 mA cm^{-2}) on the first cathodic scan to −2.25 V. However, a cathodic wave, and then a corresponding anodic wave, began to grow at a formal potential of ca. −1.75 V after a few cycles between −1.0 and −2.25 V. After 22 cycles, these waves had reached the size shown in Figure 3 and were continuing to grow. The continued growth of the n-doping waves after more than 20 cycles indicates that the n-doped state is reasonably stable. The breakin phenomenon was also observed for poly-(2,5-th$_2$py) and poly(2,5-se$_2$py) and is presumably due to restricted access of the large electrolyte cations (Bu_4N^+) to the interior of the film.[43,44] With cycling, ions and solvent would gradually accumulate within the film and facilitate doping/undoping.

Poly[2,5-bis(2-thienyl)pyridine] (poly-2). Cyclic voltammograms for two films of poly(2,5-th$_2$py) are shown in Figure 4. Again different films were used for p- and n-doping to avoid memory effects.

The p-doping electrochemistry observed in Figure 4 is similar to that previously reported for this polymer.[24] It is quite stable to potential cycling through the p-doping wave, although significant degradation was observed during impedance experiments that involved holding the film in its p-doped state for several minutes. Its p-doped form is considerably more stable than that of the 2,6-isomer (Figure 3), reflecting the more delocalized nature of the charge carriers and the resulting lower formal potential (Table 4). Surprisingly, the n-doped form of poly(2,5-th$_2$py) appears to be more stable than the p-doped form, since there was little change in the n-doping voltammetry wave following an impedance experiment on the n-doped form (Figure 4). The n-doped form was even stable in the presence of air. This is discussed further in the next section.

Poly[2,5-bis(2-selenienyl)pyridine] (poly-3). Cyclic voltammograms for two poly-(2,5-sel$_2$py) films are shown in Figure 5. For p-doping, the anodic charge passed on the forward scan was always much larger than the cathodic charge on the reverse scan. This indicates that an irreversible overoxidation process accompanies p-doping. With an upper potential limit of +1.2 V, the anodic charge decreased on consecutive scans, while the cathodic charge remained approximately constant, indicating that the p-doped form is reasonably stable at low doping levels. However, when the upper potential limit was extended to +1.5 V, no cathodic current was observed on the reverse scan and then much lower currents were observed on the subsequent anodic scan. Clearly, the p-doped form of poly-(2,5-sel$_2$py) is very easily deactivated by overoxidation.

In contrast, the n-doped form of poly(2,5-sel$_2$py) is very stable, compared with other n-doped polymers, and is even stable in the presence of air. This is illustrated in Figure 5. The final n-doping voltammogram in this figure (solid line) was recorded after more than 100 potential cycles, and holding the potential at −1.9 V for a total 150 s, all in the presence of air.

Poly[2,5-bis(1-methyl-2-pyrrolyl)pyridine] (poly-4). Cyclic voltammograms for two films of poly(2,5-mp$_2$-py) are shown in Figure 6. The voltammograms for the positive potential region, in which the upper potential limit was progressively increased from +0.7 to +1.4 V, clearly show the instability of the p-doped state. The polymer's p-doping electrochemical activity diminished and moved to higher potentials with cycling. The rate of this deactivation increases with increasing potential. Acceptable stability in the p-doped form was observed only for poly(2,5-mp$_2$py) if the potential was kept below ca. +0.80 V.

Surprisingly, poly(2,5-mp$_2$py) is reduced at a formal potential of ca. −0.8 V (Figure 6). The reduction wave decays quite rapidly with potential cycling, indicating that the reduced form is not stable.

On the basis of the lack of a reduction wave for the monomer in the potential range to −2.5 V, and the calculated high LUMO energy of the monomer, poly-(2,5-mp$_2$py) was expected to be more difficult to reduce than the other polymers studied here. The high formal potential observed for its reduction therefore suggests that this reduction does not involve the delocalized π-system. The wave shape is more characteristic of a localized reduced site than an n-doped conducting π-system (compare with Figures 3−5), supporting this

(42) Qi, Z.; Rees, N. G.; Pickup, P. G. *Chem. Mater.* **1996**, *8*, 701−707.
(43) Kaufman, F. B.; Schroeder, A. H.; Engler, E. M.; Kramer, S. R.; Chambers, J. Q. *J. Am. Chem. Soc.* **1980**, *102*, 483−487.
(44) Daum, P.; Murray, R. W. *J. Phys. Chem.* **1981**, *85*, 389−396.

Table 5. Comparison of Voltammetry Charges and Polymerization Charges in CH_3CN Containing 0.05 M Bu_4NPF_6

	p-doping		n-doping	
polymer	Q_{pol} (mC cm^{-2})	Q_{cv}/Q_{pol} (%)	Q_{pol} (mC cm^{-2})	Q_{cv}/Q_{pol} (%)
poly[2,6-bis(2-thienyl)pyridine]	64	3	80	2
poly[2,5-bis(2-thienyl)pyridine]	80	5	80	10
poly[2,5-bis(2-selenienyl)pyridine]	36	0.5	36	6
poly[2,5-bis(1-methyl-2-pyrrolyl)]pyridine]	36[a]	5	80	0.7

[a] Film prepared and measurements made in CH_3CN containing 0.1 M Et_4NClO_4.

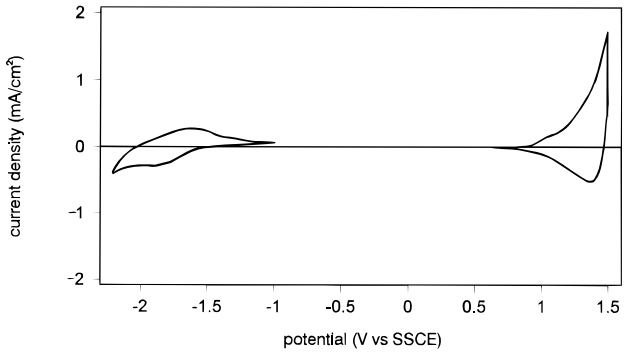

Figure 3. Cyclic voltammograms (at 100 mV s^{-1}) of two poly-[2,6-bis(2-thienyl)pyridine] (poly-**1**) coated electrodes in CH_3-CN containing 0.05 M Bu_4NPF_6. Q_{pol} values are given in Table 5. The n-doping voltammogram was recorded after 22 breakin cycles (see text).

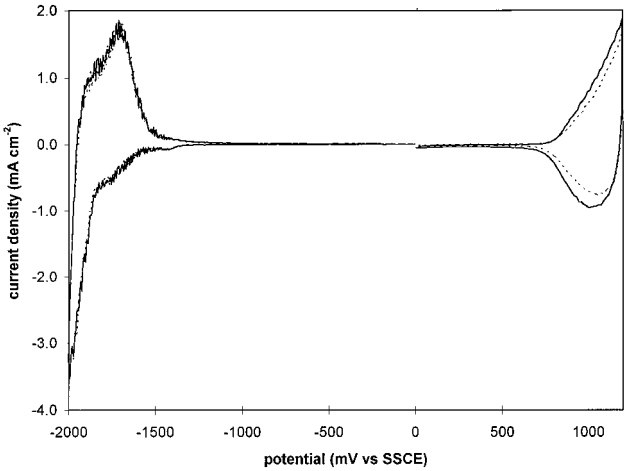

Figure 4. Cyclic voltammograms (50 or 100 mV s^{-1}) of two poly[2,5-bis(2-thienyl)pyridine] (poly-**2**) coated electrodes in CH_3CN containing 0.05 M Bu_4NPF_6. Q_{pol} values are given in Table 5. The first n-doping voltammogram (50 mV s^{-1}) was recorded after 13 breakin cycles and was stable. Dashed lines are repeat voltammograms after impedance experiments (see text).

view. The nature of this reduced state of poly(2,5-mp$_2$-py) is therefore unclear. No further reduction processes were observed in the potential range down to −2.0 V.

Conductivities. Electronic conductivities of the four polymers in their p- and n-doped states were estimated by impedance spectroscopy. Details of our interpretation of the impedance spectra of conducting polymer films and methods for extracting conductivities are given elsewhere.[23,45] Briefly, an impedance spectrum was recorded at approximately the formal potential of the appropriate redox wave, and the limiting low-frequency real impedance (minus the uncompensated solution resistance) was taken as one-third of the film's

(45) Ren, X.; Pickup, P. G. *J. Chem. Soc., Faraday. Trans.* **1993**, *89*, 321−326.

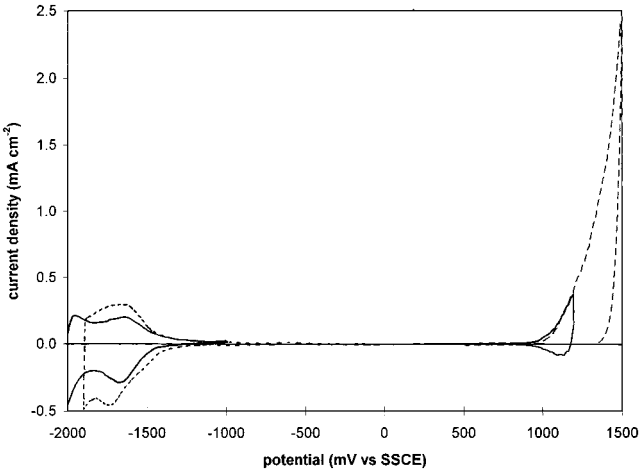

Figure 5. Cyclic voltammograms (at 100 mV s^{-1}) of two poly-[2,5-bis(2-selenienyl)pyridine] (poly-**3**) coated electrodes in CH_3-CN containing 0.05 M Bu_4NPF_6. Q_{pol} values are given in Table 5. For p-doping, the third scan to +1.2 V and a subsequent scan to +1.5 V are shown. The first n-doping (dashed line) voltammogram was recorded after ca. 30 breakin cycles and was stable. See text for details of the final n-doping voltammogram (solid-line).

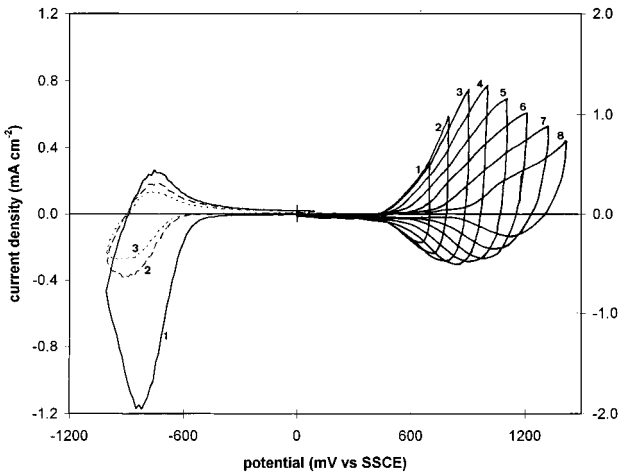

Figure 6. Cyclic voltammograms (at 100 mV s^{-1}) of two poly-[2,5-bis(1-methyl-2-pyrrolyl)pyridine] (poly-**4**) coated electrodes in CH_3CN containing 0.05 M Bu_4NPF_6. Q_{pol} values are given in Table 5. Scan numbers are indicated.

electronic resistance. A spectrum at 0 V was recorded in each case to confirm that the measured resistance was the film's electronic resistance, rather than its ionic resistance. Film thicknesses were estimated from the charge under the voltammogram, assuming a density of 1.5 g cm^{-3} and a doping level of 1 electron/three-ring monomer unit. Estimated conductivities from these experiments are given in Table 6.

The conductivities reported in Table 6 are all rather low. However, it must be remembered that the electrochemical polymerization of oligomers generally results in materials with conductivities far below intrinsic

Table 6. Estimated Conductivities from Impedance Spectroscopy for Polymers at Approximately Their Formal Potentials in CH_3CN Containing 0.05 M Bu_4NPF_6 (Film Thicknesses from 0.02 to 0.5 μm Were Used)

polymer	conductivity (S cm^{-1}) p-doped	n-doped
poly[2,6-bis(2-thienyl)pyridine]	7×10^{-6}	5×10^{-9}
poly[2,5-bis(2-thienyl)pyridine]	3×10^{-4}	1×10^{-7}
poly[2,5-bis(2-selenienyl)pyridine]	2×10^{-8}	1×10^{-7}
poly[2,5-bis(1-methyl-2-pyrrolyl)] pyridine]	5×10^{-7}[a]	4×10^{-10}

[a] Film prepared and measurements made in CH_3CN containing 0.1 M Et_4NClO_4.

values[46] and that the polymerization procedures used here were not optimized.

The conductivities obtained here for p-doped poly(2,5-th_2py) and poly(2,6-th_2py) are significantly higher than the maximum values (3×10^{-8} and 1×10^{-7} S cm^{-1}, respectively) previously reported for dry electrochemically doped samples of these materials but are significantly less than values (6 and 13 mS cm^{-1}) reported for iodine-doped samples.[3] These differences are presumably due to the instability of the electrochemically doped materials. This would lead to rapid dedoping when samples are removed from the cell and dried before conductivity measurements.

The relative conductivities of the four p-doped materials listed in Table 6 probably reflect their relative stabilities more than intrinsic differences in conductivity. The conductivities of the p-doped poly(2,5-sel_2py) and poly(2,6-th_2py) samples decreased significantly during the impedance measurements. In contrast, conductivities for the n-doped states were quite stable. The differences in n-type conductivities in Table 6 are therefore more likely to reflect differences in intrinsic conductivities, although degradation during polymerization may also be an important factor. The most notable feature of the n-type conductivities is that they are all very low relative to the p-type conductivities, despite the higher stability in the n-doped state. This indicates that the charge carriers in the n-doped states have a very low mobility, since their concentrations are reasonably high (e.g., comparable to those for the p-doped states (Table 5)). This low mobility could be due to localization of the charge carriers, or a low width of the conduction band. The decreased formal potentials observed for reduction following polymerization (Tables 1 and 4) suggest that there is significant delocalization of the n-type charge carriers.

The particularly low n-type conductivities of poly(2,6-th_2py) and poly(2,5-mp_2py) are notable. For poly(2,5-mp_2py) this provides further evidence that the reduced sites are localized (see above). For poly(2,6-th_2py), the low n-type conductivity was probably due to the low doping level of the sample (Table 5).

Conclusions

This survey of the electronic/electrochemical properties of compounds **1**−**4** and their polymers has revealed a number of problems that will severely limit the value of these materials. The instability of the p-doped states rules out applications as p-type conductors and means that oxidative polymerization will result in degraded materials. The low conductivities of the n-doped states are not attractive for applications as n-type conductors.

Because of the potential for pyridine containing conducting polymers to bind transition-metal ions and thereby form the basis for a new class of electronic materials, it is important that the origins of these problems are identified and understood. It may then be possible to design new polymers, with increased stability and conductivity, or to select appropriate transition-metal ions that will stabilize the p-doped state and increase n-type conductivity.

On a more positive note, the stability of the n-doped states observed here is encouraging, as is the relatively high conductivity observed for p-type poly(2,5-th_2py) despite its instability. This latter result, together with the literature result of 10^{-2} S cm^{-1} for an I_2-doped sample that would also have been degraded during preparation, suggests that high intrinsic conductivities are possible for pyridine containing polymers.

Acknowledgment. Financial support from the Natural Sciences and Engineering Research Council of Canada (NSERC) and Memorial University is gratefully acknowledged. We would also like to thank Raymond Poirier and Jolanta Lagowski for advice on the computational work and Neale Rees for assistance with some of the electrochemical experiments.

CM960207K

(46) Roncali, J. *Chem. Rev.* **1992**, *92*, 711−738.